

PAPER • OPEN ACCESS

Corticomuscular integrated representation of voluntary motor effort in robotic control for wrist-hand rehabilitation after stroke

To cite this article: Ziqi Guo *et al* 2022 *J. Neural Eng.* **19** 026004

View the [article online](#) for updates and enhancements.

You may also like

- [Millimeter Light Curves of Sagittarius A* Observed during the 2017 Event Horizon Telescope Campaign](#)
Maciek Wielgus, Nicola Marchili, Iván Martí-Vidal et al.
- [A Universal Power-law Prescription for Variability from Synthetic Images of Black Hole Accretion Flows](#)
Boris Georgiev, Dominic W. Pesce, Avery E. Broderick et al.
- [Broadband Multi-wavelength Properties of M87 during the 2017 Event Horizon Telescope Campaign](#)
The EHT MWL Science Working Group, J. C. Algaba, J. Anczarski et al.



PAPER

OPEN ACCESS

RECEIVED
27 October 2021

REVISED
22 January 2022

ACCEPTED FOR PUBLICATION
22 February 2022


PUBLISHED
9 March 2022

Original content from
this work may be used
under the terms of the
[Creative Commons
Attribution 4.0 licence](#).

Any further distribution
of this work must
maintain attribution to
the author(s) and the title
of the work, journal
citation and DOI.



Corticomuscular integrated representation of voluntary motor effort in robotic control for wrist-hand rehabilitation after stroke

Ziqi Guo^{1,2,5}, Sa Zhou^{1,2,5}, Kailai Ji^{1,2}, Yongqi Zhuang^{1,2}, Jie Song^{1,2}, Chingyi Nam^{1,2}, Xiaoling Hu^{1,2,3,4,*} 
and Yongping Zheng^{1,2,4}

¹ Department of Biomedical Engineering, The Hong Kong Polytechnic University, Hong Kong, People's Republic of China

² University Research Facility in Behavioral and Systems Neuroscience (UBSN), The Hong Kong Polytechnic University, Hong Kong, People's Republic of China

³ The Hong Kong Polytechnic University Shenzhen Research Institute, Shenzhen, People's Republic of China

⁴ Research Institute for Smart Ageing (RISA), The Hong Kong Polytechnic University, Hong Kong, People's Republic of China

⁵ These authors contributed equally to this work.

* Author to whom any correspondence should be addressed.

E-mail: xiaoling.hu@polyu.edu.hk

Keywords: stroke rehabilitation, robotic control, hand functions, corticomuscular coherence, voluntary motor effort

Abstract

Objective. The central-to-peripheral voluntary motor effort (VME) in the affected limb is a dominant force for driving the functional neuroplasticity on motor restoration post-stroke. However, current rehabilitation robots isolated the central and peripheral involvements in the control design, resulting in limited rehabilitation effectiveness. This study was to design a corticomuscular coherence (CMC) and electromyography (EMG)-driven control to integrate the central and peripheral VMEs in neuromuscular systems in stroke survivors. **Approach.** The CMC-EMG-driven control was developed in a neuromuscular electrical stimulation (NMES)-robot system, i.e. CMC-EMG-driven NMES-robot system, to instruct and assist the wrist-hand extension and flexion in persons after stroke. A pilot single-group trial of 20 training sessions was conducted with the developed system to assess the feasibility for wrist-hand practice on the chronic strokes (16 subjects). The rehabilitation effectiveness was evaluated through clinical assessments, CMC, and EMG activation levels. **Main results.** The trigger success rate and laterality index of CMC were significantly increased in wrist-hand extension across training sessions ($p < 0.05$). After the training, significant improvements in the target wrist-hand joints and suppressed compensation from the proximal shoulder-elbow joints were observed through the clinical scores and EMG activation levels ($p < 0.05$). The central-to-peripheral VME distribution across upper extremity (UE) muscles was also significantly improved, as revealed by the CMC values ($p < 0.05$). **Significance.** Precise wrist-hand rehabilitation was achieved by the developed system, presenting suppressed cortical and muscular compensation from the contralesional hemisphere and the proximal UE, and improved distribution of the central-and-peripheral VME on UE muscles. ClinicalTrials.gov Register Number NCT02117089

1. Introduction

Stroke is a leading cause of long-term motor disability among adults [1]. Up to 85% of stroke survivors suffer from permanent motor impairments in their hand and wrist joints [2], presenting the muscle weakness, spasticity, and muscle discoordination in the upper extremity (UE) at the chronic

stage [3]. The wrist-hand joints typically experienced a poorer and delayed motor recovery compared to the proximal joints (shoulder and elbow) in the paretic UE, lacking the long-term rehabilitation as other joints due to the limited professional manpower in the traditional physical therapy [4]. Therefore, alternative and effective techniques for the wrist-hand motor restoration are needed to improve

the independence in activities of daily living after stroke.

The central-to-peripheral voluntary motor effort (VME) in physical practice of the paretic limb is a dominant force for driving the functional neuroplasticity on motor restoration post-stroke [2]. It promotes the descending excitation from the motor cortex to the target muscle, not limited to the cortical excitation alone in voluntary motor intention [5]. Rehabilitation robots can assist the physical practice post-stroke with the advantages of higher repetition and lower costs compared with the manual therapy [6]. The rehabilitation robots that are driven by users' voluntary inputs have exhibited more significant efficacy than those with continuous passive motions (CPMs), i.e. the robots dominated the motion without users' voluntary inputs [7]. Among them, the central-intention-driven and the peripheral-effort-driven are the two main strategies of robotic control [8, 9]. Central-intention-driven systems mainly adopted the brain computer interface (BCI) technique [8]. It captured the cortical activity, typically via electroencephalography (EEG) over the sensorimotor cortex, during the mental rehearsal of movements without actual execution, i.e. motor imagery (MI) [10]. Visual or motion rewards would be provided by external devices, such as the computer screen, robots, and neuromuscular electrical stimulation (NMES), once recognized the required MI patterns [11]. MI was found to share similar cortical activation patterns with motor execution, e.g. activating the contralateral supplementary motor area, in previous functional magnetic resonance imaging (fMRI) studies [11]. Meanwhile, BCI-MI intervention has been successful on severely impaired persons, e.g. those with tetraplegia after spinal cord injury [12], because it directly bypassed the peripheral neuromuscular pathways. However, BCI-MI was little effective once the baseline voluntary physical training in routine practices, e.g. the conventionally physical and occupational therapies, was removed, and no significant differences were observed compared with the usual care or intensive care clinically [13]. In previous randomized control trials, compared to the passive motion, BCI-MI failed to enhance the motor recovery in subacute stroke persons without the voluntary physical training during the intervention, while the significantly enhanced motor recovery was only observed in the chronic stroke with the baseline voluntary physical training during the intervention [14]. BCI-MI also exhibited less effectiveness than the BCI-MI incorporated with motor attempts, where subjects were encouraged to move the paretic limb even if they had lost precise voluntary control [11]. Compared to the BCI-MI with motor attempts, the less rehabilitation effectiveness of the BCI-MI was mainly because that the pure MI without motor execution failed to promote the descending corticospinal excitation on target muscles [11]. Nonetheless, the

BCI-MI with motor attempts still failed to suppress the cortical compensation, e.g. the disinhibited contralesional hemisphere after the intervention to the hand joints [15], which could lead to muscular discoordination and limit the long-term restoration in the target muscle [16]. In this regard, the motor restoration post-stroke requires not only the volitional control in the central motor system, but also effective projection of motor commands to target muscles, i.e. central-to-peripheral VME, thereby enhancing the desired corticomuscular pathways, based on the principle of Hebbian plasticity [17, 18]. Consequently, the central-intention-driven robots had limited effectiveness on restoring the target muscle and suppressing the cortical compensation, mainly due to the central-to-peripheral VME being overlooked in the control design.

In peripheral-effort-driven robots, the electromyography (EMG) in residual muscles has been the most frequently used bio-representation of VME from the peripheral neuromuscular system in control design [19], with the EMG amplitude approximately proportional to the muscular output force [4]. It has the advantages of higher signal intensity and being less affected by the cancellation effects due to muscular discoordination post-stroke, compared to kinetic/kinematic parameters on joint/limb dynamics [7]. However, the involuntary EMG component due to spasticity post-stroke, usually triggered by the passive stretch in the compensatory motion or the release difficulty in prior contractions, could misdrive the robot by the abnormally increased EMG levels even without VME [20]. The spasticity post-stroke was non-cortically originated but rather related to the disinhibited alpha motor neurons in the descending pathways mainly originating from the brainstem [21], due to the loss of descending inputs from the cerebral cortex and basal ganglia [22]. The spastic co-contraction in compensatory motions post-stroke, e.g. the proximal-to-distal UE compensation, could lead to additional motor gains in the proximal UE even if only the distal joint was trained [16]. However, the proposed EMG processing methods to discriminate the spastic EMG lacked the validation on the cortical control for its accuracy [21], e.g. the sample entropy analysis assumed that voluntary EMGs had higher entropy than the spastic EMGs [23]. Meanwhile, reducing the compensatory motion in physical training post-stroke has relied on human supervision and manual corrections, with disadvantages of high labour demand and inaccuracy for subtle compensatory motions [16, 24]. Consequently, current peripheral-effort-driven robots have not been successful in distinguishing the cortical-originated VME from the involuntary spasticity in the control design, contributing to the insignificant advantage compared to the manual-physical therapy even with higher repetitions [22]. In this regard, incorporating the cortical-originated central-to-peripheral VME in

the control design could improve the robotic rehabilitation effectiveness.

The central and peripheral involvements were still isolated in current robots for stroke rehabilitation. Although a few EEG and EMG-driven hybrid BCI systems have recently emerged for stroke rehabilitation [25, 26], they still possessed the disadvantages of both techniques stated above, e.g. misdriving the robot with involuntary EMGs in MI without central-to-peripheral VME. Meanwhile, no significantly improved rehabilitation effectiveness in the hybrid BCI systems was reported than either the EEG- or EMG-driven strategy [25]. This was because the central-to-peripheral VME was still overlooked in these hybrid BCI systems, as the functional correlation between EEG and EMG was not considered in the decision-level fusion of the separately calculated EEG and EMG features [25, 26]. On the other hand, the cortical-originated peripheral VME can be verified by corticomuscular coherence (CMC) [27]. It demonstrates the intensity of the neural synchrony between the cortical and muscle activities during voluntary movements based on the spectral correlation between EEG and EMG (i.e. EEG-EMG coherence), with the advantage of economical computation for real-time processing [28, 29]. CMC has been conventionally applied for the evaluation of functional connection between the cortex and muscles during isometric muscle contractions, with the location of the peak CMC representing the cortical centre for the motor control to the target muscle [30]. It has also been successfully applied for evaluation on motor impairments after stroke in the literature, e.g. the decreased intensity and relocation of the peak CMC were related to the severity of motor impairments post-stroke [28, 29]. CMC has been adopted as a reliable measure of the cortical control to target muscles with a high temporal resolution in dynamic muscular efforts [29]. For example, the peak CMC location in voluntary movements was reported to be consistent with the optimal cortical motor point of the transcranial magnetic stimulation evoking the largest EMG responses on target muscles in stroke persons [28, 31]. It is possible that the cortical-originated central-to-peripheral VME could be integrated into the robotic control by introducing the CMC index, so that the robotic misdrive could be minimized due to the independency between the EEG and involuntary EMG in voluntary motor control. However, CMC was mainly used for evaluation, or diagnosis with the offline processing in previous works [32, 33]. It has not been well studied as a driving input for the online robotic control, nor the related efficacy in post-stroke rehabilitation. Therefore, the purpose of this study was to design a novel CMC-EMG-driven control to integrate the VMEs from the central and peripheral neuromuscular systems in stroke survivors through the synchronized CMC and EMG activation levels in isometric muscular contraction. In this work,

the CMC-EMG-driven control was developed in an NMES and robotic system for wrist-hand rehabilitation after stroke, and a pilot single-group trial was conducted to evaluate its feasibility and rehabilitation effectiveness for wrist-hand practices in the chronic stroke. The combined assistance of NMES and robot was to activate the agonist muscle and concurrently assist the joint kinematics with desired trajectories in wrist-hand movements [6].

2. Method

The CMC-EMG-driven NMES-robot system (figure 1(A)) was developed to instruct and assist the wrist-hand extension and flexion tasks for persons after stroke. The corticomuscular-integrated representation of VME was captured by CMC and EMG activation levels for motion recognition and system control, for the purpose of promoting the stroke persons exerting central-and-peripheral integrated VME on the target muscles. During the device-assisted wrist-hand practice, a user would receive motion instruction on a screen. The NMES-robot of the wrist-hand joint would be triggered to assist the target motions, i.e. wrist-hand extension or flexion, once the desired central-to-peripheral VME levels were detected. The pilot single-group trial was conducted with the developed system and the rehabilitation effectiveness was evaluated through clinical assessments, CMC, and EMG activation levels on chronic stroke.

2.1. CMC-EMG-driven NMES-robot system

2.1.1. System setup

Figure 1(B) depicts the system diagram with a closed-loop feedback control, which was coordinated based on a self-developed LabVIEW platform (LABVIEW 2015, National Instruments Corp.) by a personal computer (CPU: Intel (R) Core (TM) i5-9400; Windows 7 \times 64; RAM: 8.00 Gb). It consists of the functions of EEG and EMG signal acquisition and processing, visual instruction on the target motion, and motion feedback by the NMES-robot in real-time. For the EEG acquisition, a 64-channel EEG cap referenced to the left earlobe and grounded at AFz (g.GAMMAsys active electrode system, g.tec medical engineering GmbH.) was used to detect 15-channel EEG signals from the sensorimotor cortex (i.e. Cz, CPz, FCz, C1-4, CP1-4, and FC1-4), which was the main origin of central-to-peripheral VME even for stroke persons with cortical or subcortical impairments [28, 34]. The EEG signals were amplified 10 000 times (g.USBamp, g.tec medical engineering GmbH.) and band-pass filtered from 2 to 100 Hz with a 50 Hz notch filter. For the EMG acquisition, two-channel EMG signals (EMG electrode: Blue SensorN, Ambu Inc.) were captured from the muscle union of the extensor carpi ulnaris (ECU) and the extensor digitorum (ED), i.e. ECU-ED, and

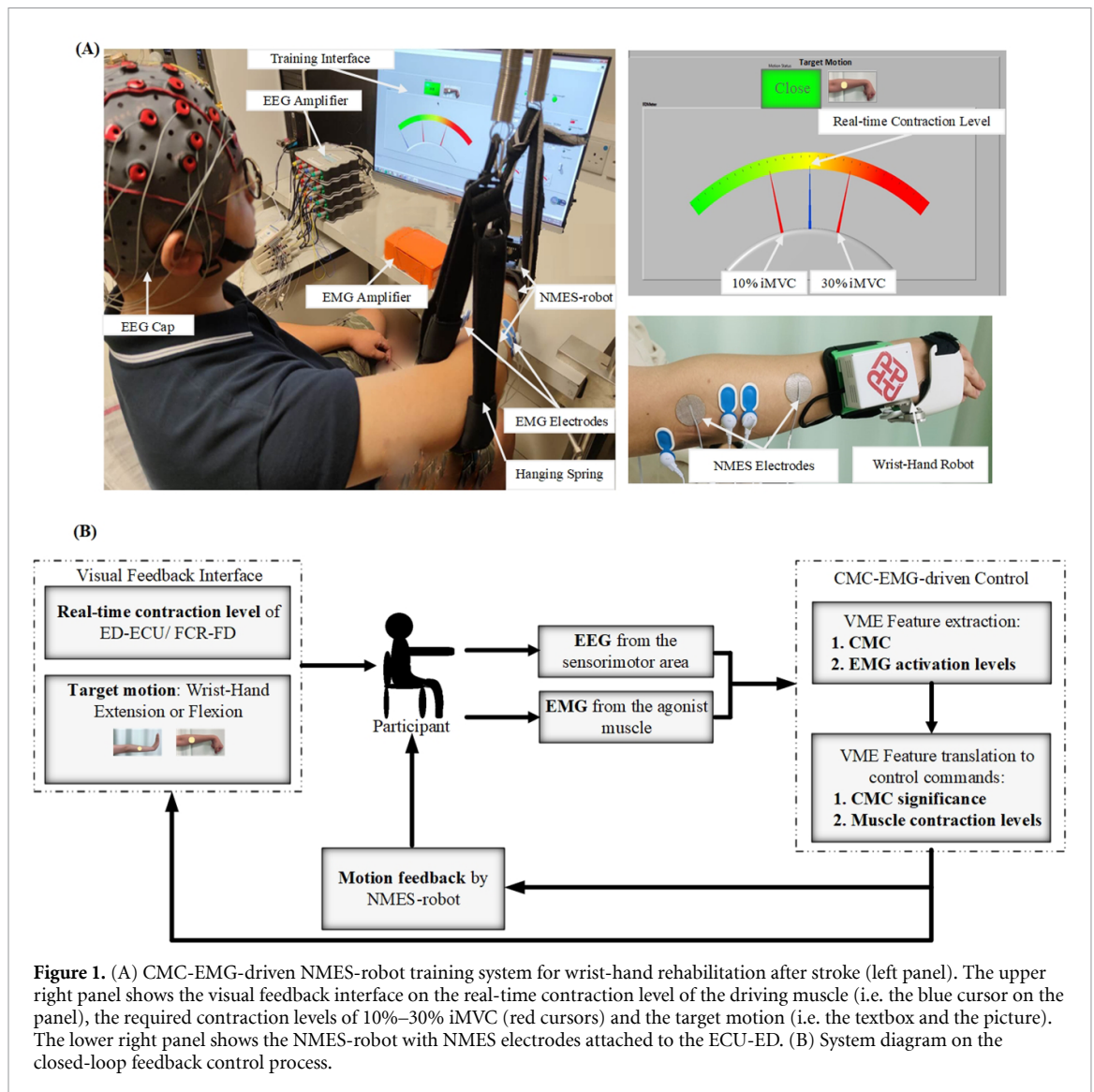


Figure 1. (A) CMC-EMG-driven NMES-robot training system for wrist-hand rehabilitation after stroke (left panel). The upper right panel shows the visual feedback interface on the real-time contraction level of the driving muscle (i.e. the blue cursor on the panel), the required contraction levels of 10%–30% iMVC (red cursors) and the target motion (i.e. the textbox and the picture). The lower right panel shows the NMES-robot with NMES electrodes attached to the ECU-ED. (B) System diagram on the closed-loop feedback control process.

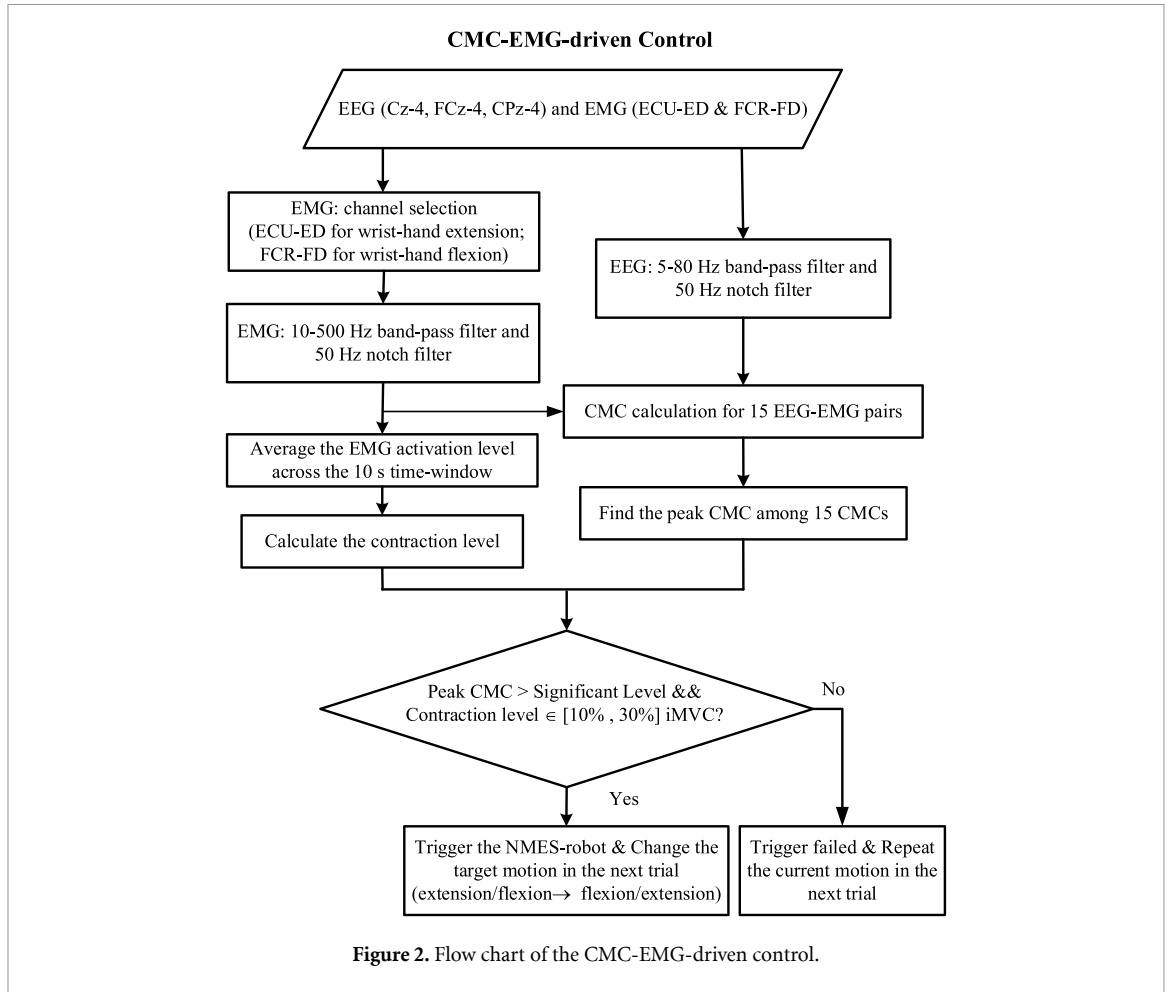
the muscle union of flexor carpi radialis (FCR) and the flexor digitorum (FD), i.e. FCR-FD, in the respective wrist-hand extension and flexion, with a reference EMG on the olecranon to reduce the common mode noise [4]. The ECU-ED and FCR-FD were treated as muscle unions because of their close anatomical proximity and their narrow muscle bellies [6]. EMG signals were amplified 1000 times (INA 333, Texas Instruments Inc.) and band-pass filtered from 10 to 500 Hz with a 50 Hz notch filter. A DAQ card (6218 NI DAQ card, National Instruments Corp.) was adopted to synchronize the EEG and EMG acquisition with a sampling rate of 1,200 Hz.

The NMES-robot was used to assist the wrist-hand extension or flexion with constant feedbacks for motion rewards on the central-to-peripheral VME (figure 1(A)) [6]. The robot (450 g) was a mechanical exoskeleton connected with a motor (MX 106, Trossen Robotics, with a maximal stall torque of 8.4 Nm) that provided a range of motion (ROM) from 45° in wrist extension to 60° in wrist flexion (i.e. −45° to 60°) with a constant angular velocity of 10°/s

[6]. One-channel NMES was used to provide constant electrical stimulation on ECU-ED to assist the wrist-hand extension (square pulse with adjustable pulse width of 0–300 μ s, 70 V, 40 Hz), while no NMES was provided to the FCR-FD, as practiced previously [6]. This is because the wrist-hand flexion can be achieved voluntarily in many persons with chronic stroke, and more severe impairments were typically observed in UE extensors than flexors [6]. A visual feedback interface on the computer screen was developed to provide instruction on the target motions and the real-time and desired contraction levels for isometric contraction on the target muscle (figure 1(B)).

2.1.2. CMC-EMG-driven control

The corticomuscular integrated representation of VME was designed by capturing the synchronized CMC and EMG levels in isometric muscular contraction (figure 2), representing the respective cortical-originated central-to-peripheral VME and the peripheral VME in neuromuscular systems. A triggering-mode strategy was adopted in the control



design that the desired central-to-peripheral VME levels on the agonist muscle were first detected using the real-time EEG and EMG in a triggering time window of 10 s when the user maintaining the target motion before actuating the NMES-robot. The real-time desired central-to-peripheral VME was identified by the significant peak CMC in the sensorimotor area and the EMG activation level in the agonist muscle within 10%–30% of its isometric maximal voluntary contraction (iMVC) level in the 10 s window. Once detected the desired central-to-peripheral VME levels, the NMES-robot would be triggered to assist the target motion for motion rewards, i.e. trigger success, the subject would be instructed not to exert VME (i.e. receive the passive motion), and the system would not capture EEG and EMG either. Otherwise, the NMES-robot would not be triggered, i.e. trigger failed, and the current target motion would be repeated in the next trial.

The real-time estimation of CMC was based on the coherence between the 15-channel EEG from the sensorimotor cortex (i.e. Cz, CPz, FCz, C1-4, CP1-4, and FC1-4) and the one-channel EMG from the agonist muscle unit (ECU-ED or FCR-FD) in the 10 s window. The triggering time window of 10 s was selected to ensure the stationarity of EEG and EMG, as well as the statistical power of the CMC

significant level in real-time control. It was also to improve the sustainability of VME generation in isometric contraction, due to the impaired postural stability post-stroke [16]. The CMC between the EEG from the sensorimotor cortex $x_{\text{EEG}}(t)$ and the EMG in the agonist muscle $x_{\text{EMG}}(t)$ was calculated in the beta band (15–30 Hz) as follows [29]:

$$\text{CMC} = \frac{|S_{\text{EEG,EMG}}(f)|^2}{S_{\text{EEG,EEG}}(f) * S_{\text{EMG,EMG}}(f)} \quad (1)$$

where $S_{\text{EEG,EEG}}(f)$ and $S_{\text{EMG,EMG}}(f)$ are the respective auto-spectrums of EEG and EMG. $S_{\text{EEG,EMG}}(f) = \langle X_{\text{EEG}}(f) X_{\text{EMG}}^*(f) \rangle$ is the cross-spectrum between the EEG and EMG, where $X_{\text{EEG}}(f)$ and $X_{\text{EMG}}(f)$ are the respective Fourier transforms of $x_{\text{EEG}}(t)$ and $x_{\text{EMG}}(t)$, * indicates the complex conjugate and $\langle \rangle$ is the expectation value. The EEG and EMG were further pre-processed (EEG: 5–80 Hz band-pass filter and 50 Hz notch filter; EMG: 10–500 Hz band-pass filter and 50 Hz notch filter), and then segmented into epochs of 1024 points with 50% overlap, i.e. time windows of 853 ms with 426 ms shifts, generating 22 epochs in a 10 s triggering time window before the CMC calculation [20]. The largest CMC value among the 15 EEG channels was selected as the peak CMC. The significance of the peak CMC, i.e. the significant

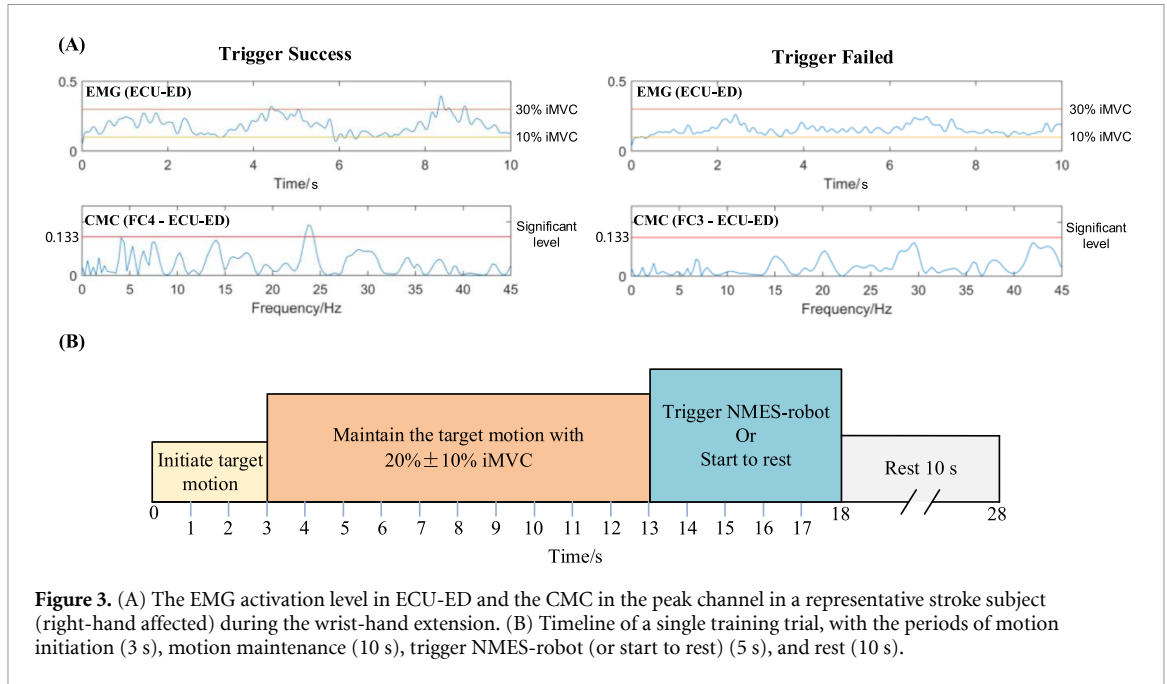


Figure 3. (A) The EMG activation level in ECU-ED and the CMC in the peak channel in a representative stroke subject (right-hand affected) during the wrist-hand extension. (B) Timeline of a single training trial, with the periods of motion initiation (3 s), motion maintenance (10 s), trigger NMES-robot (or start to rest) (5 s), and rest (10 s).

CMC level, was estimated through the coherence confidence level $CL_{(\alpha\%)}$ as follows [29]:

$$CL_{(\alpha\%)} = 1 - P^{\frac{1}{N-1}} \quad (2)$$

where $P = 0.05$ is the statistical significance level (i.e. $\alpha = 95$), $N = 22$ is the number of epochs, and $CL_{(\alpha\%)} = 0.133$. A peak CMC above the confidence level $CL_{(\alpha\%)}$ was considered to be significant [35].

The EMG activation level in the real-time control of the NMES-robot was calculated based on the one-channel EMG from the agonist muscle in the 10 s window. The mean EMG activation level $EMG_{Activation}$ was obtained by taking the average of the real-time EMG activation level (i.e. 100 ms moving average for the rectified EMG) over the 10 s [6]. It was normalized to be the corresponding contraction level as follows [29]:

$$EMG_{Contraction} = \frac{EMG_{Activation} - EMG_{Base}}{EMG_{Max} - EMG_{Base}} \quad (3)$$

where EMG_{Max} and EMG_{Base} , representing the respective 100% iMVC and 0% iMVC, are the respective maximum and resting state $EMG_{Activation}$ in the iMVC test [29]. The iMVC test was conducted at the beginning of each training session, which will be described in section 2.3 Training protocol. The system delay used for the CMC and EMG activation level calculation was 10–15 ms, which could be ignored in the motion control by the stroke persons who had a slow pace [4, 6].

The trigger failed could be detected in the following three cases: (a) No significant CMC but a desired EMG activation level (i.e. within the 10%–30% iMVC) could be observed in the ‘incorrect’ compensatory motions or muscular spasticity after stroke.

(b) No desired EMG activation level but a significant CMC could be observed when the target muscle was overactivated or less activated ($EMG_{Activation} > 30\%$ or $< 10\%$ iMVC). The muscular overactivation was typically observed due to the higher perceived difficulty in lower contraction levels, which is related to the impaired fine motor control after stroke [2]. (c) Neither significant CMC nor desired EMG activation level was observed when there was no voluntary contraction and no spasticity in the subject. Figure 3(A) shows the representative EMG envelope (i.e. the EMG activation level) in ECU-ED and the CMC in the peak channel (right-hand affected) in a stroke subject during wrist-hand extension. When the trigger success occurred (figure 3(A), left panel), there was a significant peak CMC in the mid-beta band (20–25 Hz) and the mean EMG activation level was within the desired 10%–30% iMVC. In contrast, when trigger failed (figure 3(A), right panel), the case (a) was observed that no significant CMC was found at any frequency, although there were desired EMG activation levels.

Visual instruction on the real-time EMG activation levels, the required EMG activation range, and the required motion states (wrist-hand extension or flexion, or rest) was provided to the user, as shown in figure 1(A) (upper right panel). The real-time EMG activation level was displayed by the blue cursor on the screen. The desired contraction level was 20% iMVC (i.e. the midline in the panel) with an acceptable error range of $\pm 10\%$ iMVC (i.e. the two fixed red cursors), to ensure that the mean EMG activation level over the 10 s triggering time window could vary within the required range of 10%–30% iMVC. The 20% iMVC was selected in the real-time control, for the purpose of improving the fine motor control

Table 1. Demographic data of the stroke participants.

Participant	Gender Female/ Male	Age (years)	Onset Years	Stroke Type Hemorrhage/ Ischemic	Affected Side Right/Left
S1	F	67	7	Hemorrhage	Right
S2	F	51	8	Ischemic	Left
S3	F	63	2	Ischemic	Left
S4	F	59	1	Ischemic	Right
S5	F	66	5	Hemorrhage	Left
S6	M	63	7	Ischemic	Right
S7	M	67	14	Hemorrhage	Right
S8	M	57	5	Hemorrhage	Right
S9	M	57	10	Hemorrhage	Left
S10	M	58	8	Ischemic	Left
S11	M	47	11	Ischemic	Right
S12	M	53	8	Ischemic	Left
S13	M	45	4	Hemorrhage	Right
S14	M	54	3	Hemorrhage	Left
S15	M	65	7	Ischemic	Left
S16	M	66	9	Hemorrhage	Right
Overall	5/11	58.6 \pm 7.1	6.8 \pm 3.4	8/8	8/8

on the wrist-hand joints post-stroke [16]. This was because that the lower-level contractions required more motor efforts and cognitive concentration in the force output than the higher-level contractions [32]. Another reason was that the sustained contraction with moderate levels (<50% iMVC) was achievable for persons after stroke. It can evoke evident CMC in the beta band and avoid muscle fatigue in continuous contractions when compared with the higher levels [16].

2.2. Subject recruitment

This study was approved by the Human Subjects Ethics Subcommittee of The Hong Kong Polytechnic University (approval number: HSEARS20170502002; HSEARS20190119001), which was in accordance with the Declaration of Helsinki and local statutory requirements. The stroke subjects recruited in this study satisfied the following inclusion criteria: (a) 45–70 years old; (b) ≥ 1 year after the onset of unilateral brain lesions due to subcortical stroke, without other neurological impairments or secondary onset [36]; (c) no visual, cognitive or attentional deficits (mini-mental state examination score > 21) to ensure that the subject could understand and follow instructions during the experiment [37]; (d) moderate to severe motor impairments on the unilateral UE (Fugl-Meyer assessment for UE (FMA-UE) score of $15 < \text{FMA-UE} < 45$, with a maximal score of 66) [38]; (e) Modified Ashworth Scale (MAS) < 3 for the muscle tone at the elbow, wrist, and fingers [39]; (f) detectable voluntary EMG (i.e. three times standard deviation above the baseline) from ECU-ED, FCR-FD, TRI and BIC in the affected limb. Finally, sixteen stroke subjects (Age, 58.6 ± 7.1 years;

Stroke onset, 6.8 ± 3.4 years) were recruited and completed the training, as detailed in the demographic data in table 1. All participants were informed of the research purpose and provided their written consent.

2.3. Training protocol

The recruited subjects were invited to attend the pilot single-group trial to evaluate the rehabilitation effectiveness of the developed system. The training comprised 20 training sessions, with 3–5 sessions per week within seven consecutive weeks. Each session lasted 1.5 h, not including the preparation time, as adopted previously [4]. The subjects were required not to attend any other rehabilitation programs until the three month follow-up. All the recruited subjects ($n = 16$) completed the training sessions.

At the beginning of each session, each participant was invited to sit comfortably in front of the computer screen. The EEG cap was mounted onto the scalp according to the 10–20 system. Two-channel EMG electrodes were attached to the common area of the muscle bellis of the antagonist muscle pairs, ECU-ED and FCR-FD, with the reference electrode attached to the surface of the olecranon (figure 1(A)). The impedance of each EEG and EMG electrode was prepared below 5 k Ω [29]. Then, the iMVC test was conducted on the target muscles, ECU-ED and FCR-FD, to obtain their $\text{EMG}_{\text{Max}-i}$ and $\text{EMG}_{\text{Base}-i}$ for EMG normalization (i.e. equation (3)) in the CMC-EMG-driven control, which could minimize the deviation effects caused by positioning EMG electrodes across the training sessions [40]. The subject was instructed to (a) keep the testing upper limb relaxed to obtain

the baseline EMG, (b) execute the iMVC in wrist-hand flexion to obtain the maximum EMG on FCR-FD, and (c) execute the iMVC in wrist-hand extension to obtain the maximum EMG on ECR-ED [16]. The wrist joint was positioned at 0° and the elbow joint was at 90° during the test [16]. Each iMVC test was performed for 5 s and repeated thrice with a 5 min break between two consecutive iMVCs to avoid muscle fatigue. The EMG_{Max-i} and EMG_{Base-i} in a muscle were calculated as the respective mean EMG activation level (as in the section 2.1.2 CMC-EMG-driven control) over the baseline and iMVC tests [29]. After the iMVC test, the NMES electrode pair was attached to the common area of the ECU-ED with perpendicular to the EMG electrodes (figure 1(A), lower right panel), as practiced in our previous work [6]. The NMES pulse width was identified to evoke maximal wrist extension and full finger extension, which was the highest tolerable threshold personally without pain sensation and muscle fatigue in the training [6]. Then, the robot module of the device was fixed on the wrist-hand joint using a bracing system with adaptive pressures on the skin [6]. A hanging system was used to lift the testing limb up to a horizontal level for gravity compensation on the limb and the NMES-robot. Also, the testing hand was placed in a neutral position to make the force output plane orthogonal to the gravity. The initial and terminal positions of the wrist joint were at 45° extension, with the elbow joint kept at 180° extension in a training trial.

During the training, each subject was instructed to perform the target motions, wrist-hand extension and flexion, on the visual feedback interface (figure 1(A)). The timing of a training trial is shown in figure 3(B). The subject was required to initiate the target motion to the required contraction level within 3 s after the motion onset, and maintain it for 10 s, that is, keep the blue cursor at the panel midline (i.e. the desired 20% iMVC) with an allowable fluctuation within the two fixed red cursors (i.e. $\pm 10\%$ iMVC) (figure 1(A)). After the 13 s motion phase, the subject would immediately receive the motion assistance by the NMES-robot if generated the desired central-and-peripheral VME levels as mentioned in section 2.1.2 CMC-EMG-driven control. Otherwise, the subject would bring forward to rest and be instructed to repeat and the target motion in the next trial. The intertrial rest was 10 s with a 2 min break between 10 consecutive trials (~ 4.6 min) to avoid muscle fatigue. The subject was asked to minimize body movements, eye blinking, biting, and to avoid falling asleep or engaging in active mental tasks during the target motions. The raw EEG and EMG signals were stored for offline analysis, in addition to the online processing in section 2.1.2 CMC-EMG-driven control. Muscle fatigue was monitored by the experimenter according to the EMG mean power frequency (MPF) [41],

and no fatigue was found across trials ($<10\%$ MPF reduction).

2.4. Evaluation on rehabilitation effectiveness

2.4.1. Cross-sessional variation of CMC topography and trigger success rate

The hemispheric dominance, i.e. lateralization, was investigated by the laterality index (LI) of CMC across training sessions. The LI was a typical measure for the hemispheric asymmetry in the topographical distribution in fMRI and EEG studies [42, 43]. In this work, it was applied to quantify the relative contribution of the ipsilesional hemisphere to the contralesional hemisphere and the central area in the CMC topography, which was calculated as follows:

$$LI = \frac{CMC_{ipsilesional}}{\max(CMC_{contralesional}, CMC_{midsagittal\ plane})} \quad (4)$$

where $CMC_{ipsilesional}$ and $CMC_{contralesional}$ are the respective peak CMC value among the nine EEG channels in the ipsilesional hemisphere (e.g. FC1 3 5, CP1 3 5, and C1 3 5 for the right-hand affected) and in the contralesional hemisphere (e.g. FC2 4 6, CP2 4 6, and C2 4 6 for the right-hand affected). The $CMC_{midsagittal\ plane}$ is the peak CMC value among the three channels in the midsagittal plane (i.e. FCz, Cz, and CPz). The LI was calculated for trials with trigger success across training sessions, with the same CMC estimation as in section 2.1.2. The trigger success rate was calculated as the proportion of the number of trigger success trials to the total number of trials on the wrist-hand extension or flexion in a training session.

2.4.2. Clinical assessments

The rehabilitation effectiveness was evaluated through clinical assessments, i.e. MAS at the elbow, wrist, and fingers [39], action research arm test (ARAT) [44], and FMA for the upper limb [38]. The FMA (full score: 66) was also sub-scaled into shoulder/elbow (42/66) and wrist/hand (24/66). The clinical assessments were performed three times in two weeks before the training (Pre-training) with an interval of 2–3 days for baseline stability, once immediately after the last training session (Post-training), and once at three months after the training (3FU), by a blinded assessor. The FMA was adopted as the primary outcome measure in this work [11].

2.4.3. Evaluation by CMC and EMG activation levels

The rehabilitation effectiveness on the central-and-peripheral integration of VME post-stroke was evaluated by CMC and EMG activation levels in isometric wrist-hand extension and flexion at the contraction levels of 20% iMVC and 40% iMVC, denoted as 20% Ex, 40% Ex, 20% Fx and 40% Fx [29]. The motion scheme at 40% iMVC was also used to evaluate the rehabilitation effectiveness on the tasks with lower perceived difficulty than the target level of 20% iMVC

in the training protocol [16, 45]. The evaluation sessions were conducted one day before and after the training sessions.

In the evaluation setup, the testing forearm was placed on a horizontal fixed slab in the neutral position with the force output plane orthogonal to the gravity [29]. The acquisition and amplification setup of EEG and EMG were the same as the section 2.3 Training protocol. In addition to the ECU-ED and FCR-FD, two-channel EMG electrodes were attached to the antagonist muscle pairs for elbow extension and flexion, i.e. triceps (TRI) brachii and bicep (BIC) brachii, to investigate the proximal-to-distal compensation in the UE post-stroke [16]. Visual feedback on the target motion, the real-time contraction level, and the required contraction range was provided to the subject, as in section 2.3 Training protocol (figure 1(A), upper right panel). The required contraction levels were 20% iMVC and 40% iMVC with an acceptable error range of $\pm 10\%$ iMVC.

At the beginning of the evaluation, the iMVC test on each muscle (i.e. ECU-ED, FCR-FD, BIC and TRI) was conducted with procedures similar to those in section 2.3 Training protocol. After the iMVC test, the subject conducted the four target motion schemes, 20% Ex, 40% Ex, 20% Fx and 40% Fx, in a random order. The subject was required to initiate the motion to the target level within 3 s and keep the blue cursor at the panel midline (the 20% or 40% iMVC) for 35 s with an allowable fluctuation within the two fixed red cursors ($\pm 10\%$ iMVC). Each motion scheme was repeated five times with a 2 min rest between two consecutive contractions to avoid muscle fatigue [16]. The muscle fatigue was checked immediately after each trail using the EMG MPF as in section 2.3 Training protocol [29], and no fatigue was detected across the trials. EEG and EMG signals were simultaneously recorded and stored for offline analysis. The EEG and EMG were then pre-processed for denoising with procedures as in our previous works [16]. Finally, CMC and EMG activation levels were calculated for the EEG and EMG with respect to different muscles in the four motion schemes using equations (1)–(3). The LI of CMC was also calculated for each agonist muscle in the four motion schemes with equation (4).

2.5. Statistics

After the Shapiro-Wilk test of normality, each variable, i.e. the clinical scores, LI, CMC, and the EMG activation level, was confirmed to obey the normal distribution ($P > 0.05$). One-way analysis of variance (ANOVA) with the Bonferroni post hoc test was used to evaluate the mean difference of LI and trigger success rate across every five training sessions (i.e. session 1–5, 6–10, 11–15, and 16–20), and to evaluate the mean difference of clinical scores across different time points (i.e. the pre-training, post-training, and 3FU assessments). A paired t-test was performed on the CMC and EMG activation levels by comparing the

difference between the pre-training and post-training evaluation. The level of statistical significance was set at 0.05, which was also indicated at 0.01 and 0.001. All statistical analyses in this study were performed using SPSS 24.0 (2016).

3. Results

3.1. Cross-sessional variation of CMC topographies

Figure 4(A) shows the cross-sessional CMC topographies on ECU-ED during the wrist-hand extension in a representative stroke subject (right hemiparesis) with the respective trigger success and trigger failed of the NMES-robot, where 10 sessions were illustrated among the total 20 sessions. When trigger success, the CMC peak channel presented a shift pattern from the contralesional (right) to the ipsilesional (left) sensorimotor area from session 1 to session 19. The CMC peak channel was in the contralesional sensorimotor area (CP2) in session 1, and then it shifted to the ipsilesional sensorimotor area in sessions 3, 5, and 7 (CP1, CP3, and FC1, respectively). Although the peak channel was in the contralesional sensorimotor area (CP2) in session 9, it was in the ipsilesional sensorimotor area in all last sessions (session 11: C1; sessions 13 and 15: CP3; sessions 17 and 19: FC3). This shift pattern, as quantified by the LI of CMC, presented an increase from the $LI < 1$ to $LI > 1$ from the session 1 to session 19. The LI was 0.70 in session 1 and then increased to > 1 in sessions 3, 5, 7, and 11 (1.11, 1.09, 1.01 and 1.01, respectively). Although session 9 had $LI = 0.94$, all of the last sessions 13–19 had an $LI > 1.1$ (1.27, 1.18, 1.13, and 1.31 in sessions 13, 15, 17, and 19, respectively). In contrast to the trigger success, when the trigger failed, the peak channels were in the contralesional hemisphere and the respective LIs were < 1 in all sessions except sessions 3 and 5 (peak channel: CP1; $LI > 1$).

Figure 4(B) summarizes the mean LI on ECU-ED across all trigger success trials and the mean trigger success rate across every five sessions in the representative subject during the wrist-hand extension. Table 2 lists the detailed LI values and the trigger success rate presented with means and standard deviations, in addition to the one-way ANOVA probability and the effect size (EF). Significantly increased LI was observed after the first five sessions, i.e. sessions 1–5 ($p < 0.01$ for sessions 6–10 and 16–20, $p < 0.05$ for session 11–15, one-way ANOVA with Bonferroni post-hoc test). Meanwhile, the trigger success rate was significantly increased from 68% to 90% after the session 1–5 ($p < 0.05$ for session 6–10, 11–15, and 16–20, one-way ANOVA with Bonferroni post-hoc test). Figure 4(C) presents the group-level LI of CMC on the agonist muscle in the target motion schemes, 20% Ex, 40% Ex, 20% Fx, and 40% Fx, before and after the training. Table 3 lists the detailed LI values presented with means and standard deviations, in addition

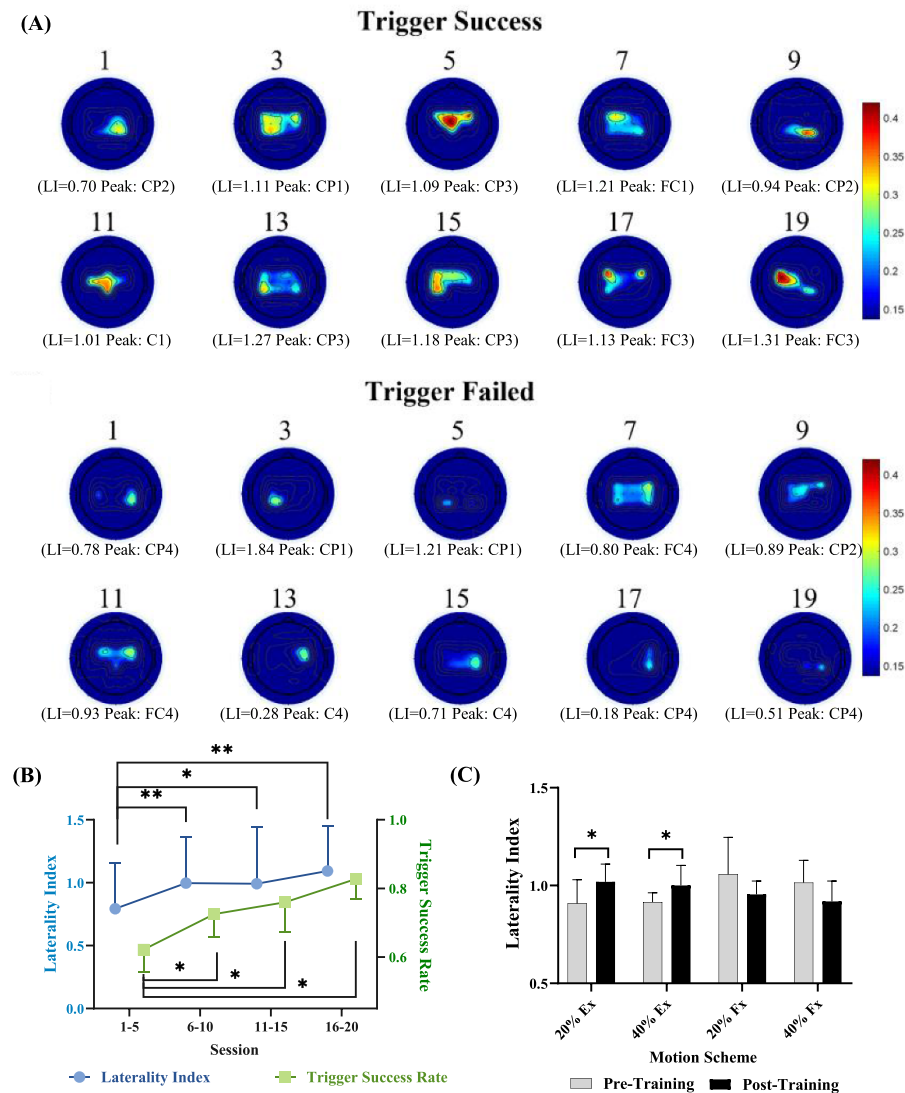


Figure 4. (A) Cross-sectional CMC topographies on ECU-ED in a representative stroke subject (right-hand affected) during the wrist/hand extension. The color scheme indicates the CMC value in each channel. The laterality index (LI) and the peak channel of CMC are indicated below the topography, with the session number above the topography. (B) Averaged LI on ECU-ED in all trigger success trails and the respective trigger success rate across every five training sessions in the representative subject during the wrist/hand extension. (C) LI of CMC on the agonist muscle during the target motion schemes, i.e. 20% Ex, 40% Ex, 20% Fx, and 40% Fx, in all subjects before and after the training. The LI and the trigger success rate are presented as the mean and standard deviation (error bar). Significant differences with respect to the training sessions and motion schemes are indicated as ‘*’ for $P < 0.05$ and ‘***’ for $P < 0.01$.

to the paired t-test probabilities and the EFs. Significantly increased LI was observed at 20% and 40% Ex after the training ($p < 0.05$, EF = 0.748 at 20% Ex and EF = 0.741 at 40% Ex, paired t-test). In contrast, no significant increase of LI was found at either 20% or 40% Fx after the training ($p > 0.05$, EF = 0.673 at 20% Fx and EF = 0.624 at 40% Fx, paired t-test).

3.2. Training effects on clinical scores

Figure 5 summarizes the motor improvements measured by clinical scores (i.e. the FMA, ARAT, and MAS scores) before, after, and three month after the training. Table 4 lists the detailed clinical scores presented with means and standard deviations, in addition to

the one-way ANOVA probabilities and the EFs. Significant increases were observed in the FMA wrist/hand score (figure 5(A); $p < 0.05$, EF = 0.242, one-way ANOVA with the Bonferroni post hoc test) and the ARAT score (figure 5(C); $p < 0.01$, EF = 0.522, one-way ANOVA with the Bonferroni post hoc test) after the training, and these increases were maintained after three months. Meanwhile, significant decreases were observed in the MAS scores at the finger (figure 5(D); $p < 0.01$, EF = 0.504, one-way ANOVA with the Bonferroni post hoc test) and the wrist (figure 5(E); $p < 0.001$, EF = 0.597, one-way ANOVA with the Bonferroni post hoc test), and these decreases were maintained after three months. By contrast, no significant variation was found in the

Table 2. Laterality Index of CMC and trigger success rate across the 20 training sessions with respect to the ECU-ED in a representative subject (right hemiparesis) during wrist/hand extension.

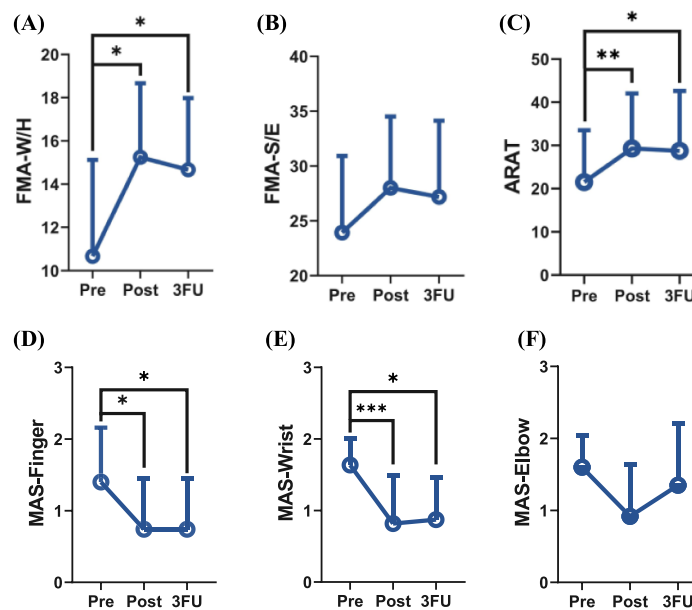
Parameter \ Session number	Session number				One-way ANOVA
	1–5	6–10	11–15	16–20	P (Partial η^2)
Laterality index (Mean \pm SD)	0.79 \pm 0.36	0.99 \pm 0.36	0.99 \pm 0.45	1.09 \pm 0.35	0.001** (0.059)
Trigger Success Rate (Mean \pm SD)	0.68 \pm 0.06	0.73 \pm 0.07	0.76 \pm 0.09	0.90 \pm 0.06	0.001** (0.546)

The superscript * indicates the significant difference across training sessions (one-way ANOVA with the Bonferroni post hoc test), with 1 superscript for $P < 0.05$ and two superscripts for $P < 0.01$.

Table 3. Laterality Index of CMC with respect to the agonist muscle in all subjects during the four motion schemes before and after the training.

Motion scheme \ Evaluation time point	Motion scheme			
	20% Ex	40% Ex	20% Fx	40% Fx
	Laterality index (Mean \pm SD)			
Pre-training	0.91 \pm 0.12	0.92 \pm 0.05	1.06 \pm 0.19	1.01 \pm 0.11
Post-training	1.02 \pm 0.09	1.00 \pm 0.10	0.95 \pm 0.07	0.92 \pm 0.10
Paired t-test	0.04*	0.04*	0.06	0.08
P (Cohen's d)	(0.748)	(0.741)	(0.673)	(0.624)

The superscript * indicates the significant difference with $P < 0.05$.

**Figure 5.** Variation of clinical scores measured before (Pre) and after the training (Post), as well as at the three month follow-up (3FU): (A) FMA wrist/hand scores, (B) FMA shoulder/elbow scores, (C) ARAT scores (D-F) MAS scores at the fingers, wrist, and elbow. The clinical scores are presented as means and standard deviations (error bars) at each assessment time point. The significant difference across assessment time points is indicated as ‘*’ for $P < 0.05$, ‘**’ for $P < 0.01$, and ‘***’ for $P < 0.001$.

FMA shoulder/elbow score (figure 5(B); $p > 0.05$, EF = 0.068, one-way ANOVA with the Bonferroni post hoc test) and the MAS elbow score (figure 5(F); $p > 0.05$, EF = 0.153, one-way ANOVA with the Bonferroni post hoc test) across the assessment time points.

3.3. Training effects on CMC and EMG activation levels

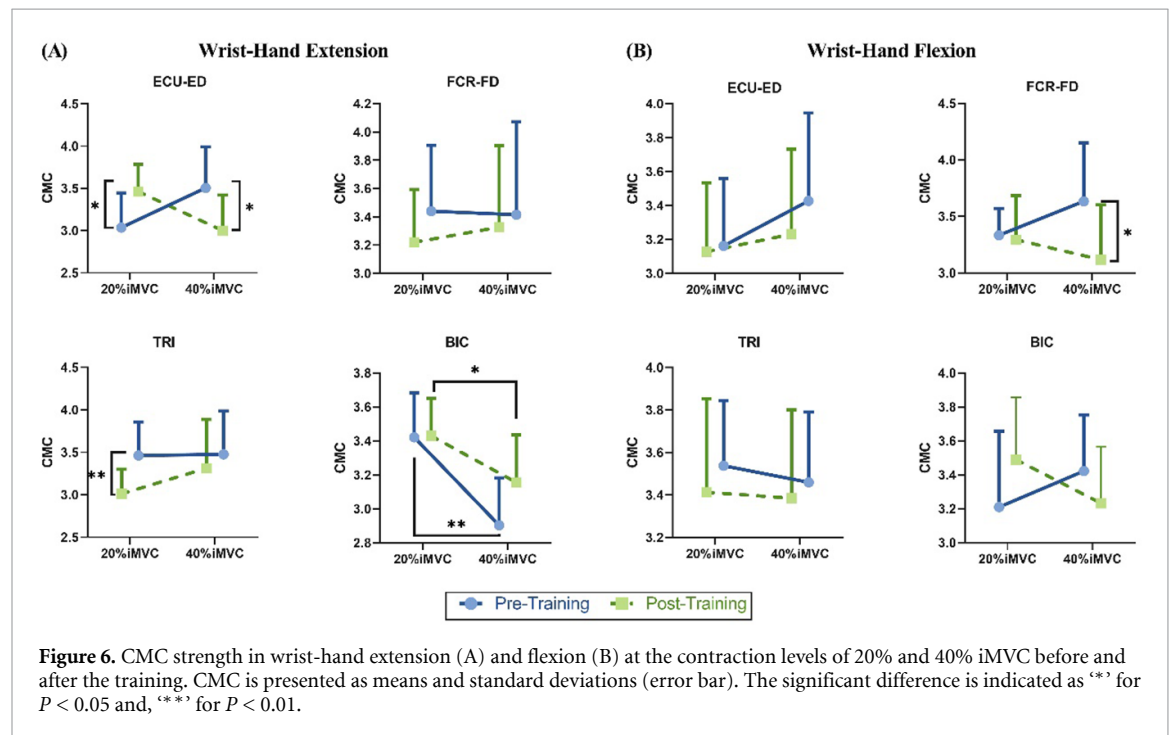
Figure 6 shows the CMC on UE muscles in the four motion schemes, 20% Ex, 40% Ex, 20% Fx and 40%

Fx, before and after the training. Tables 5 and 6 list the detailed CMC values presented with the means and standard deviations, in addition to the paired t-test probabilities and the estimated EFs. In the wrist-hand extension (figure 6(A), table 5), the ECU-ED showed a significantly increased CMC at 20% Ex ($p < 0.05$, EF = 1.415, paired t-test) and a significantly decreased CMC at 40% Ex ($p < 0.05$, EF = 0.971, paired t-test) after the training. The TRI showed a significantly decreased CMC at 20% Ex ($p < 0.01$, EF = 1.724, paired t-test), with no significant change

Table 4. Clinical scores before, after and three month after the CMC-EMG-driven NMES-robot training.

Evaluation (Max Score)	Pre-training	Post-training	Three month FU	One way ANOVA
	Clinical score (Mean \pm SD)			P (Partial η^2)
FMA Wrist/Hand (24)	10.66 \pm 4.45	15.25 \pm 3.41	14.66 \pm 3.31	0.010* (0.242)
FMA Shoulder/Elbow (42)	23.91 \pm 6.99	28.00 \pm 6.50	27.16 \pm 6.96	0.315 (0.068)
FMA Full Score (66)	34.58 \pm 10.97	43.25 \pm 9.44	41.83 \pm 9.39	0.089 (0.173)
ARAT (57)	21.50 \pm 12.02	29.33 \pm 12.71	28.75 \pm 13.89	0.002** (0.522)
MAS Finger (4)	1.25 \pm 0.80	0.81 \pm 0.66	0.78 \pm 0.64	0.002** (0.504)
MAS Wrist (4)	1.67 \pm 0.37	0.87 \pm 0.66	1.05 \pm 0.83	0.000*** (0.597)
MAS Elbow (4)	1.60 \pm 0.44	0.92 \pm 0.72	1.35 \pm 0.85	0.065 (0.153)

The superscript * indicates the significant difference regarding the training effects (one-way ANOVA with the Bonferroni post hoc test), with 1 superscript for $P < 0.05$, 2 superscripts for $P < 0.01$, and three superscripts for $P < 0.001$. Three month FU, three month follow-up assessment; SD, standard deviation; FMA, Fugl-Meyer Assessment [38]; MAS, Modified Ashworth Scale [39]; ARAT, Action Research Arm Test [44].



at 40% Ex ($p > 0.05$, EF = 0.190, paired t-test) after the training. No significant CMC change was found in the flexors FCR-FD and BIC at either 20% or 40% Ex after the training ($p > 0.05$, paired t-test). In addition, a significant difference between the two contraction levels, 20% and 40% iMVCs, was observed in BIC with significantly higher CMCs at 20% Ex than 40% Ex both before and after the training ($p < 0.05$, EF = 1.627 in pre-training and EF = 1.358 in post-training, paired t-test). No significant CMC difference between 20% Ex and 40% Ex was found in ECU-ED, FCR-FD, and TRI ($p > 0.05$, paired t-test). In the wrist-hand flexion (figure 6(B), table 6), the FCR-FD had a significantly decreased CMC at 40% Fx ($p < 0.05$, EF = 1.030, paired t-test), without significant change at 20% Fx ($p > 0.05$, EF = 0.137, paired t-test) after the training. There was no significant CMC difference in the ECU-ED, TRI, and BIC with respect to either the evaluation time points or the contraction levels ($p > 0.05$, paired t-test).

Figure 7 presents the training effects on EMG activation levels in the wrist-hand extension and flexion at 20% and 40% iMVCs. Table 7 lists the detailed EMG activation levels presented with the means and standard deviation, in addition to the paired t-test probabilities and the estimated EFs. At 20% Ex (figure 7(A)), significantly decreased EMG activation levels were observed in TRI ($p < 0.05$, EF = 1.007, paired t-test), without significant change in BIC and FCR-FD ($p > 0.05$, EF = 0.273 in BIC and EF = 0.531 in FCR-FD, paired t-test) after the training. At the 40% Ex (figure 7(B)), significantly decreased EMG activation levels were observed in the flexors BIC and FCR-FD ($p < 0.05$, EF = 0.905 in BIC and EF = 1.101 in FCR-FD, paired t-test), without significant change in the TRI ($p > 0.05$, EF = 0.644, paired t-test) after the training. At 20% Fx (figure 7(C)), significantly increased EMG activation levels were observed in the ECU-ED ($p < 0.05$, EF = 0.926, paired t-test), without significant change in the BIC and TRI ($p > 0.05$,

Table 5. CMC on UE muscles during the wrist-hand extension at different contraction levels before and after the training.

Muscle	Evaluation time point	20% Ex	40% Ex	Paired t-test
		CMC (Mean* 100 \pm SD)		P (Cohen's d)
ECU-ED	Pre-training	3.04 \pm 0.41	3.51 \pm 0.48	0.113 (0.784)
	Post-training	3.46 \pm 0.32	2.99 \pm 0.42	0.108 (0.924)
	Paired t-test	0.018*	0.042*	
	P (Cohen's d)	(1.415)	(0.971)	
FCR-FD	Pre-training	3.44 \pm 0.46	3.41 \pm 0.65	0.897 (0.047)
	Post-training	3.22 \pm 0.37	3.33 \pm 0.57	0.676 (0.228)
	Paired t-test	0.419	0.255	
	P (Cohen's d)	(0.328)	(0.476)	
TRI	Pre-training	3.46 \pm 0.39	3.47 \pm 0.51	0.875 (0.075)
	Post-training	3.01 \pm 0.29	3.31 \pm 0.57	0.580 (0.269)
	Paired t-test	0.002**	0.608	
	P (Cohen's d)	(1.724)	(0.190)	
BIC	Pre-training	3.42 \pm 0.26	2.90 \pm 0.28	0.011* (1.627)
	Post-training	3.43 \pm 0.22	3.15 \pm 0.28	0.012* (1.358)
	Paired t-test	0.945	0.204	
	P (Cohen's d)	(0.027)	(0.540)	

The superscript * indicates the significant difference of $P < 0.05$ with respect to the training effects and different contraction levels.

Table 6. CMC on UE muscles during the wrist-hand flexion at different contraction levels before and after the training.

Muscle	Evaluation time point	20% Fx	40% Fx	Paired t-test
		CMC (Mean* 100 \pm SD)		P (Cohen's d)
ECU-ED	Pre-training	3.16 \pm 0.40	3.43 \pm 0.52	0.103 (0.726)
	Post-training	3.13 \pm 0.41	3.23 \pm 0.50	0.609 (0.204)
	Paired t-test	0.897	0.389	
	P (Cohen's d)	(0.047)	(0.324)	
FCR-FD	Pre-training	3.34 \pm 0.47	3.63 \pm 0.517	0.273 (0.456)
	Post-training	3.29 \pm 0.39	3.12 \pm 0.484	0.764 (0.118)
	Paired t-test	0.709	0.022*	
	P (Cohen's d)	(0.137)	(1.030)	
TRI	Pre-training	3.54 \pm 0.31	3.46 \pm 0.33	0.795 (0.124)
	Post-training	3.41 \pm 0.44	3.39 \pm 0.42	0.629 (0.234)
	Paired t-test	0.618	0.756	
	P (Cohen's d)	(0.198)	(0.114)	
BIC	Pre-training	3.21 \pm 0.45	3.42 \pm 0.33	0.847 (0.092)
	Post-training	3.49 \pm 0.37	3.27 \pm 0.37	0.220 (0.517)
	Paired t-test	0.258	0.546	
	P (Cohen's d)	(0.472)	(0.264)	

The superscript * indicates the significant difference of $P < 0.05$ with respect to the training effects and different contraction levels.

EF = 0.289 in BIC and EF = 0.166 in TRI, paired t-test) after the training. At 40% Fx (figure 7(D)), significantly decreased EMG activation levels were observed in the BIC ($p < 0.05$, EF = 0.887, paired t-test), without significant change in the extensors, ECU-ED and TRI ($p > 0.05$, EF = 0.309 in ECU-ED and EF = 0.368 in TRI, paired t-test) after the training.

4. Discussion

The CMC-EMG-driven NMES-robot system was developed with corticomuscular integrated representation of VME for the wrist-hand rehabilitation after stroke. A pilot trial was conducted to evaluate the feasibility and rehabilitation effectiveness of the developed system on those

with chronic strokes. It was found that the CMC-EMG-driven control was effective for the wrist-hand practice post-stroke, presenting the improved corticomuscular integration of VME and the guided cortical neuroplasticity across training sessions. The training effects on clinical scores, CMC, and EMG activation levels demonstrated that the developed system achieved precise wrist-hand improvements, reduced compensation from the proximal UE and the contralesional hemisphere, and improved distribution of the central-and-peripheral VME on UE muscles.

4.1. Feasibility of the CMC-EMG-driven control

The CMC-EMG-driven control in the NMES-robot system was feasible to instruct and assist the wrist-hand practice, presenting improved

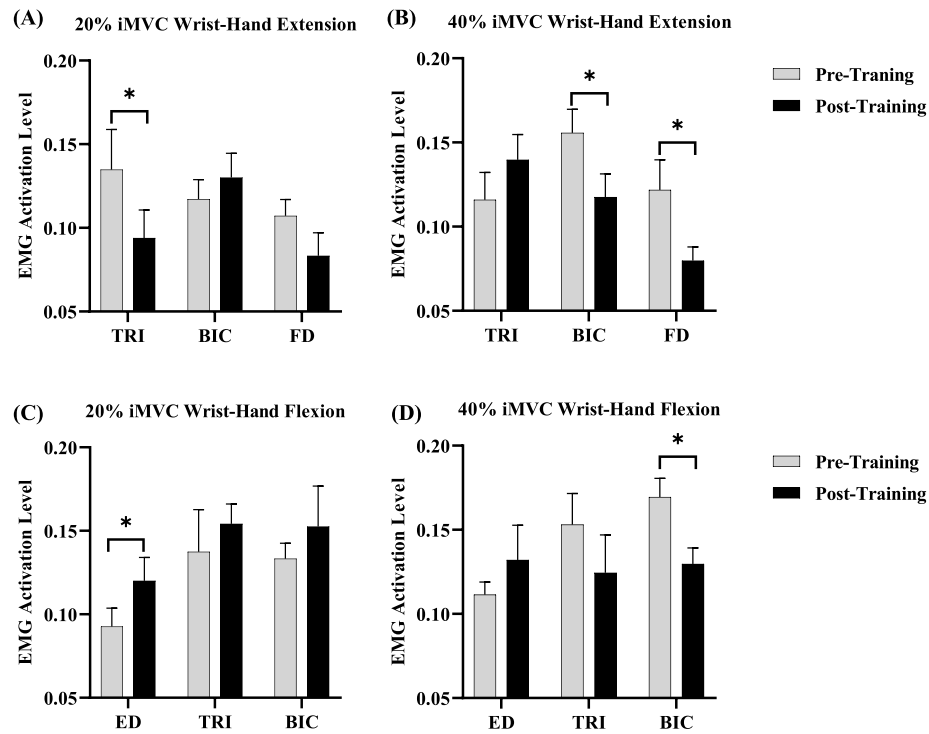


Figure 7. EMG activation levels in the target motion schemes, (A) 20% Ex, (B) 40% Ex, (C) 20% Fx and (D) 40% Fx, before and after the training, presented as means and standard deviations (error bars). The significant difference before and after the training is indicated as ‘*’ for $P < 0.05$.

Table 7. EMG activation levels on UE muscles during the wrist-hand extension and flexion at different contraction levels before and after the training.

		Wrist-hand extension			Wrist-hand flexion		
		TRI	BIC	FCR-FD	ECU-ED	TRI	BIC
Contraction level	Evaluation time point	EMG activation level (Mean \pm SD)					
20% iMVC	Pre-training	0.14 \pm 0.07	0.12 \pm 0.04	0.11 \pm 0.03	0.93 \pm 0.03	0.14 \pm 0.08	0.13 \pm 0.03
	Post-training	0.09 \pm 0.05	0.13 \pm 0.04	0.08 \pm 0.04	0.12 \pm 0.04	0.15 \pm 0.04	0.15 \pm 0.07
	Paired t-test	0.017*	0.437	0.150	0.024*	0.632	0.411
	P (Cohen's d)	(1.007)	(0.273)	(0.531)	(0.926)	(0.166)	(0.289)
40% iMVC	Pre-training	0.12 \pm 0.05	0.16 \pm 0.04	0.12 \pm 0.05	0.11 \pm 0.02	0.15 \pm 0.05	0.17 \pm 0.03
	Post-training	0.14 \pm 0.05	0.12 \pm 0.04	0.08 \pm 0.02	0.13 \pm 0.06	0.12 \pm 0.06	0.13 \pm 0.03
	Paired t-test	0.090	0.027*	0.011*	0.410	0.333	0.040*
	P (Cohen's d)	(0.644)	(0.905)	(1.101)	(0.309)	(0.368)	(0.887)

The superscript * indicates the significant difference with $P < 0.05$.

corticomuscular integration of VME and guided cortical neuroplasticity in stroke persons. This was revealed by the significantly increased trigger success rate and the shifted CMC peak channel from the contralesional to the ipsilesional hemisphere in wrist-hand extension across the 20 training sessions (figures 4(A) and (B)), where the reduced compensation from the contralesional hemisphere implied motor restoration to the targeted wrist-hand joint [46]. The significantly increased trigger success rate tended to be stable after 6–10 sessions. Meanwhile, the stroke participants verbally reported that they could control the ‘learned-disused’ muscles (ECU-ED and FCR-FD) and could achieve the required level (20% \pm 10% iMVC) much easier

after two consecutive weeks of training, i.e. 6–8 sessions. In addition, the increased trigger success rate was accompanied by enhanced hemispheric lateralization in wrist-hand extension, as quantified by the significantly increased LI after 6–10 sessions (figure 4(B)), which was absent in wrist-hand flexion after the training. It suggested that the improved corticomuscular integration of VME could guide the cortical neuroplasticity on wrist-hand extension in the CMC-EMG-driven control, because of the corticospinal re-innervation to the targeted wrist-hand muscles, as detailed in section 4.3. In this work, the trigger success rate of the CMC-EMG-driven control was higher than the BCI-MI-based control in the chronic stroke, e.g. $66 \pm 25.7\%$ [47]. It implied

that the CMC-EMG-driven system could be more reliable for VME recognition to engage more voluntary inputs and to provide more feedback than the BCI-MI system. This was possibly because of the low accuracy and the required user-specific adaptation in the event-related desynchronization-based motion recognition during the MI practice [20].

The 10 s triggering time window in the real-time control was comparable to the BCI-MI systems for stroke rehabilitation [10], e.g. 6 s [13] and 7 s [48] for motor imagery, although it was longer than the EMG-driven system, e.g. 100 ms [49]. In addition to ensuring the EEG and EMG stationarity and the statistical power of the CMC significant level, the 10 s window could improve the stability and sustainability of VME generation in isometric contraction after stroke, due to their impaired postural stability related to the muscle weakness, spasticity, and muscle discoordination [50].

4.2. Training effectiveness on wrist-hand functions

Motor restoration on the targeted wrist-hand joint was determined by the improved voluntary motor functions, released spasticity, and finer precision control on grasping, gripping, and pinching motions. These were revealed by significant changes of the FMA wrist/hand scores (figure 5(A)), the MAS finger and wrist scores (figures 5(D) and (E)), and the ARAT scores (figure 5(C)) after the training and at the three month follow-up [44]. Among the FMA subscales, the improved stability of wrist extension, i.e. active wrist extension with $\geq 15^\circ$ ROM and resistance tolerable, in all subjects demonstrated the effectiveness of the 10 s window in CMC-EMG-driven control on improving the sustainability of VME generation and the related postural stability. In addition, the reduced spasticity at the finger and wrist joints confirmed the effectiveness of the CMC index on eliminating the robotic 'misdrive' due to muscle spasticity in the control design. In contrast, previous BCI-MI-driven, EMG-driven, or CPM systems presented no significant release of the finger spasticity after the training, despite similar motion assistance, i.e. NMES and robot, and comparable training intensity to this work [11, 51]. Furthermore, the released spasticity at the wrist-hand joints also implied the decreased hyperexcitability of alpha motor neurons, i.e. the lower motor neuron, in the spinal cord after the training. It was because that the spasticity post-stroke was found to be related to disinhibited alpha motor neurons in the spinal cord, due to the loss of descending control in corticospinal tracts [22]. In the unimpaired, the excitability of the alpha motor neurons was effectively controlled by the descending corticospinal inputs through the presynaptic stimulation of the upper motor neurons in voluntary movements [21]. In this regard, the decreased hyperexcitability of alpha motor neurons could be related to the facilitated descending corticospinal inputs to target muscles

by the CMC-EMG-driven control after the training, which was observed from the enhanced cortical control in the ipsilesional hemisphere in the significant CMC and LI changes on target muscles as detailed in following sections.

4.3. Precise rehabilitation with reduced cortical and proximal muscular compensation

The CMC-EMG-driven NMES-robot achieved precise motor restoration on the targeted wrist-hand joint with minimized proximal-to-distal UE compensation that widely observed in previous rehabilitation trainings with either voluntary inputs or CPM. The results found no significant improvement of the proximal UE in the FMA shoulder/elbow and the MAS elbow scores (figures 5(B) and (F)). It suggested that the CMC-EMG-driven control was effective at suppressing the compensatory motion from the proximal UE in the fine motor control to the wrist-hand joints, i.e. the 20% isometric contraction in this work, without additional human supervision, manual correction or restriction to the proximal joints, as in the previous literature [2]. It was because that the corticomuscular integrated VME in limb practice facilitated the corticospinal re-innervation to the targeted wrist-hand muscles, by reducing the compensation from the proximal UE with a cortical origin in the contralesional hemisphere [16], as detailed in the following paragraph. By contrast, the additional improvements on proximal UE could be easily obtained in previous rehabilitation training on the distal UE even when the proximal UE and trunk were restricted to move by apparatus or belts, e.g. the EMG-driven NMES-robot or the passive robotic assistance [49, 52]. Although the additional improvement in the proximal joints seems to be helpful in a short-term, it could exacerbate the compensatory motion, the reduced range of joint motion, abnormal inter-joint motions, and pain, leading to maladaptive neuroplasticity after stroke [2]. In this work, the motion rewards provided by the NMES-robot to the central-to-peripheral VME could promote the motor learning on the desired motion and suppress the compensatory motion after stroke. In the control design, motion rewards from the NMES-robot were provided (i.e. trigger success) only if the subject exerted the desired central-to-peripheral VME levels, i.e. significant CMC and target EMG activation levels. Otherwise, no motion reward was provided by the NMES-robot (i.e. trigger failed) and the subject was instructed to repeat the target motion, e.g. trigger failed occurred when no significant CMC but a desired EMG activation level due to the 'incorrect' compensatory motions or muscular spasticity. The incentive scheme for motor relearning has been extensively adopted in previous BCI- or EMG-driven rehabilitation robots after stroke, based on the Hebbian plasticity [17, 49]. The effectiveness of the combined assistance of NMES-robot for motor

relearning has been reported in our previous works that it significantly improved the muscle coordination after stroke than the NMES or robot alone, reducing the ‘learned-disuse’ on the distal UE [4]. It was because that the NEMS-robot could concurrently activate the agonist muscle via the NMES and assist the joint kinematics with desired trajectories via the robot assistance, guiding the effective motor patterns in stroke persons [4].

In addition to the reduced muscular compensation, the precise wrist-hand rehabilitation with CMC-EMG-driven NMES-robot also reduced the compensation from the contralesional hemisphere after the training, i.e. the cortical guidance effect. It was revealed by the significantly increased LI of CMC in wrist-hand extension at both 20% iMVC and 40% iMVC after the training, while no significant change was found in the wrist-hand flexion at either contraction levels (figure 4(C)). The facilitated hemispheric lateralization to the ipsilesional hemisphere could re-innervate the target wrist-hand muscles by enhancing the desired ipsilesional pathways, contributing to the minimized proximal-to-distal UE compensation. In previous works, the cortical compensation has been demonstrated to be anatomically and functionally related to muscular compensation in the UE post-stroke, leading to the maladaptive neuroplasticity related to the ‘learned-disuse’ in the long-term recovery [16]. Although relocation of the peak CMC to the contralesional hemisphere was found in the distal UE movements post-stroke, this contralesional control in the cortex mainly benefited the motor functions in the proximal UE and introduced muscular discoordination among UE muscles, e.g. the flexion synergy in arm reaching and the proximal-to-distal UE compensation [16, 53]. A poorer and delayed recovery in the distal UE was commonly observed than the proximal UE and the body trunk in the chronic stroke [16], because that the spontaneous motor recovery was from the proximal to the distal joints during the first six month after stroke. Another reason was that the distal wrist-hand muscles were primarily innervated by the ipsilesional hemisphere through the decussate lateral corticospinal tracts, while the proximal UE had bi-hemispheric innervation through both the crossed dorsolateral and the uncrossed ventromedial spinal cord [16]. Despite this bi-hemispheric innervation on the proximal UE, the cortical compensation from the ipsilateral hemisphere had a lower conduction efficiency than the contralateral control to the proximal UE, due to the less-dense extrapyramidal tracts (15% pyramidal tract fibres) from the ipsilateral hemisphere than the fast pyramidal tracts (85% pyramidal tract fibres) from the contralateral hemisphere anatomically [16]. It was also found that motor restoration in the distal UE was related to the cortical control from the ipsilesional hemisphere, rather than the contralesional hemisphere, which was revealed by the increased peak

CMC intensity in the ipsilesional motor cortex after the rehabilitation training [54, 55]. For example, the ARAT scores were found to be significantly correlated with the cortical activation in the ipsilesional motor cortex, without significant correlation with the contralesional side in the chronic stroke [46]. Furthermore, the cortical guidance effect suggested that the CMC-EMG-driven strategy had superior modulatory effects on driving positive neuroplasticity over the central-intention-driven robots. A previous BCI-MI-driven hand robot failed to inhibit the CMC from the contralesional hemisphere in stroke persons after the training [15]. It could imply a lack of precise rehabilitation to the distal UE in the BCI-MI-driven strategy, due to the correlation between the disinhibited contralesional hemisphere and the proximal-to-distal UE compensatory motion [16, 53, 55].

4.4. Improved central-and-peripheral VME in wrist-hand movements

Improved distribution of the peripheral VME on UE muscles directly validated the precise wrist-hand improvements and the reduced proximal-to-distal UE compensation, as observed from the significant changes in the EMG activation levels (figure 7). There was significantly improved extensor weakness (ECU-ED, figure 7(C)), significantly released flexor spasticity (FCR-FD, figure 7(B)) and significantly reduced excessive activation in proximal muscles (BIC and TRI, figures 7(A), (B), and (D)) after the training, which was consistent with the findings in the FMA, ARAT, and MAS scores (figure 5). The improved extensor weakness demonstrated that the CMC-EMG-driven strategy could be more effective for reducing the ‘learned-disuse’ on wrist-hand extensors than the peripheral-effort-driven strategy. It was because that, in the EMG-driven NMES-robot, the UE extensors typically experienced a poorer recovery compared to the significantly released flexor spasticity [6, 49]. For example, in the EMG-driven exoneuromusculoskeleton, the muscle activation level in UE extensors, ECU-ED and TRI, had no significant increase in the arm reaching and withdrawing with hand opening and grasping tasks, despite the comparable training intensity and similar assistance to this work [49].

Improved distribution of the central-to-peripheral VME on UE muscles was achieved in the precise wrist-hand rehabilitation with minimized compensation from the proximal muscles, particular in the fine motor control of finger extension, 20% Ex. In the results, significant CMC changes after the training were mainly observed in the agonist muscles in the distal UE, i.e. ED-ECU and FD-FCR, but without significant changes on the antagonist and most proximal muscles, e.g. BIC (figure 6). The relative high task difficulty for fine motor control on finger extension could result in the significantly reduced CMC on TRI and significantly increased

CMC on ED-ECU in 20% Ex after the training, indicating a more independent control to the target ED-ECU [16]. In contrast, no significant CMC changes on BIC in both 20% and 40% Fx and on FD-FCR in 20% Fx after the training were mainly because of the relatively low task difficulty for flexion than extension in the upper limb in the chronic stroke, particularly for the BIC in elbow flexion [4]. In addition, the difficulty-dependent training effect on the CMC pattern was also found in the improved VME distribution in the agonist muscles, which presented significantly increased CMC in the 20% Ex, but significantly reduced CMC at 40% Ex and Fx after the training. In other words, the stroke participants exerted greater central-to-peripheral VME at a relatively more difficult contraction level (20% iMVC), but reduced VME at a simpler contraction level (40% iMVC) after the training. This also demonstrated that the CMC-EMG-driven control with the required contraction level of 20% iMVC could benefit multiple mild-to-moderate contraction levels, i.e. 20% and 40% iMVC, thereby contributing to the precise wrist-hand rehabilitation. It was because that the corticomuscular integrated VME exerted in a higher perceived difficulty task (20% iMVC) could engage additional corticospinal tracts and somatosensory afferents for more proprioceptive feedback and finer motor control, as suggested previously in unimpaired persons [45]. On the other hand, the NMES assistance combined with the CMC-EMG-driven control could facilitate the central-to-peripheral VME on the target ECU-ED at 20% iMVC through the sensorimotor integration [43]. It was because that >50% stroke persons experienced the sensory deficiency with proprioception disturbance and increased uncertainty on the peripheral states in voluntary motion [43]. The rich sensory input of NMES on the desired muscle location, joint position, and the movement trajectory reduced these uncertainties and facilitated effective motor patterns in motion practice post-stroke [56]. In this work, the compensatory VME from the BIC could still exist in the wrist-hand extension, as revealed by the significantly higher CMC at 20% Ex than at 40% Ex after the training. It suggested that the proximal-to-distal UE compensation was not eliminated, despite being minimized, in the motion practice assisted by the CMC-EMG-driven NMES-robot. The difficulty-dependent CMC patterns after the training extended our knowledge on the CMC-based robotic control and evaluation on motor functions in stroke rehabilitation.

Despite no sham group in this work, the CMC-EMG-driven control achieved precise wrist-hand rehabilitation with minimized compensatory movements from the proximal UE, in comparison with the EMG-driven control to the same NMES-robot presenting additional proximal improvements in our previous works [49]. In the future work, randomized control trials will be conducted to compare

the effects of the CMC-EMG-driven control with the conventional robotic controls, e.g. the central-intention-driven, the peripheral-effort-driven, or different stimulation configurations in the NMES-robot, in parallel.

5. Conclusion

In this work, the CMC-EMG-driven NMES-robot system with corticomuscular integrated representation of VME was developed for effective wrist-hand rehabilitation by suppressing the cortical and muscular compensation after stroke. It achieved precise wrist-hand improvements, reduced compensation from the proximal UE and the contralesional hemisphere, and improved distribution of the central-and-peripheral VME on UE muscles. Specifically, the cross-session CMC variation suggested that the developed system was feasible and effective for wrist-hand practice post-stroke, as it significantly improved the corticomuscular integration of VME and guided the cortical neuroplasticity after the 6–10 training sessions. For the precise wrist-hand improvements, the proximal-to-distal UE compensation was effectively suppressed during the fine motor control of wrist-hand joints, i.e. at 20% Ex, without additional human supervision, manual correction, or restriction to the proximal joints. It could be attributed to the corticospinal re-innervation to the targeted wrist-hand muscles in the enhanced ipsilesional pathways, as revealed by the reduced compensation from the contralesional hemisphere after the training. Furthermore, in the improved central-and-peripheral VME distribution, the CMC-EMG-driven control with the required 20% iMVC benefited multiple mild-to-moderate contraction levels, i.e. 20% and 40% iMVC, as revealed by the difficulty-dependent training effect on the CMC patterns in the agonist muscles. It suggested that the developed system could engage more corticospinal tracts and somatosensory afferents for finer motor control of the wrist-hand joints, thereby contributing to the precise wrist-hand rehabilitation.

Data availability statement

The data generated and/or analysed during the current study are not publicly available for legal/ethical reasons but are available from the corresponding author on reasonable request.

Acknowledgments

The authors would like to thank the participants who participated in this study. This project was funded by the National Natural Science Foundation of China (NSFC 81771959), the University Grants Committee Research Grants Council, Hong Kong (GRF 15207120), and the Science and Technology Innovation Committee of Shenzhen, China (2021Szzvup142).

Ethical statement

The human experiments were conducted after we obtained the ethical approval from the Human Subjects Ethics Sub-Committee of The Hong Kong Polytechnic University (approval number: HSEARS20170502002 and HSEARS20190119001) and the written informed consent from all subjects. All participants are aware of the intended publication. The experiments are in accordance with the Declaration of Helsinki and local statutory requirements.

ORCID iD

Xiaoling Hu  <https://orcid.org/0000-0003-3188-3005>

References

- [1] Levin M F, Kleim J A and Wolf S L 2009 What do motor 'recovery' and 'compensation' mean in patients following stroke? *Neurorehabil. Neural Repair* **23** 313–9
- [2] Jones T A 2017 Motor compensation and its effects on neural reorganization after stroke *Nat. Rev. Neurosci.* **18** 267–80
- [3] Dewald J P, Pope P S, Given J D, Buchanan T S and Rymer W Z 1995 Abnormal muscle coactivation patterns during isometric torque generation at the elbow and shoulder in hemiparetic subjects *Brain* **118** 495–510
- [4] Hu X-L, Tong R K-Y, Ho N S, Xue J-J, Rong W and Li L S 2015 Wrist rehabilitation assisted by an electromyography-driven neuromuscular electrical stimulation robot after stroke *Neurorehabil. Neural Repair* **29** 767–76
- [5] Turton A and Lemon R 1999 The contribution of fast corticospinal input to the voluntary activation of proximal muscles in normal subjects and in stroke patients *Exp. Brain Res.* **129** 559–72
- [6] Rong W, Li W, Pang M, Hu J, Wei X, Yang B, Wai H, Zheng X and Hu X 2017 A Neuromuscular Electrical Stimulation (NMES) and robot hybrid system for multi-joint coordinated upper limb rehabilitation after stroke *J. Neuroeng. Rehabil.* **14** 1–13
- [7] Chen M, Wu B, Lou X, Zhao T, Li J, Xu Z, Hu X and Zheng X 2013 A self-adaptive foot-drop corrector using functional electrical stimulation (FES) modulated by tibialis anterior electromyography (EMG) dataset *Med. Eng. Phys.* **35** 195–204
- [8] Ang K K and Guan C 2013 Brain-computer interface in stroke rehabilitation *J. Comput. Sci. Eng.* **7** 139–46
- [9] Mukaino M, Ono T, Shindo K, Fujiwara T, Ota T, Kimura A, Liu M and Ushiba J 2014 Efficacy of brain-computer interface-driven neuromuscular electrical stimulation for chronic paresis after stroke *J. Rehabil. Med.* **46** 378–82
- [10] Chaudhary U, Birbaumer N and Ramos-Murguialday A 2016 Brain–computer interfaces for communication and rehabilitation *Nat. Rev. Neurol.* **12** 513–25
- [11] Bai Z, Fong K N, Zhang J J, Chan J and Ting K 2020 Immediate and long-term effects of BCI-based rehabilitation of the upper extremity after stroke: a systematic review and meta-analysis *J. Neuroeng. Rehabil.* **17** 1–20
- [12] Pfurtscheller G, Müller-Putz G R, Pfurtscheller J and Rupp R 2005 EEG-based asynchronous BCI controls functional electrical stimulation in a tetraplegic patient *EURASIP J. Adv. Signal Process.* **2005** 628453
- [13] Ang K K, Guan C, Chua K S G, Ang B T, Kuah C W K, Wang C, Phua K S, Chin Z Y and Zhang H 2011 A large clinical study on the ability of stroke patients to use an EEG-based motor imagery brain-computer interface *Clin. EEG Neurosci.* **42** 253–8
- [14] Bovend'Eerd T J, Dawes H, Sackley C, Izadi H and Wade D T 2010 An integrated motor imagery program to improve functional task performance in neurorehabilitation: a single-blind randomized controlled trial *Arch. Phys. Med. Rehabil.* **91** 939–46
- [15] Belardinelli P, Laer L, Ortiz E, Braun C and Gharabaghi A 2017 Plasticity of premotor cortico-muscular coherence in severely impaired stroke patients with hand paralysis *NeuroImage* **14** 726–33
- [16] Zhou S, Guo Z, Wong K, Zhu H, Huang Y, Hu X and Zheng Y-P 2021 Pathway-specific cortico-muscular coherence in proximal-to-distal compensation during fine motor control of finger extension after stroke *J. Neural Eng.* **18** 056034
- [17] Mrachacz-Kersting N, Jiang N, Stevenson A J T, Niazi I K, Kostic V, Pavlovic A, Radovanovic S, Djuric-Jovicic M, Agosta F and Dremstrup K 2016 Efficient neuroplasticity induction in chronic stroke patients by an associative brain-computer interface *J. Neurophysiol.* **115** 1410–21
- [18] Zhou S, Xie P, Chen X, Wang Y, Zhang Y and Du Y 2018 Optimization of relative parameters in transfer entropy estimation and application to corticomuscular coupling in humans *J. Neurosci. Methods* **308** 276–85
- [19] Takahashi C D, Der-Yeghiaian L, Le V, Motiwala R R and Cramer S C 2008 Robot-based hand motor therapy after stroke *Brain* **131** 425–37
- [20] Chowdhury A, Raza H, Meena Y K, Dutta A and Prasad G 2019 An EEG-EMG correlation-based brain-computer interface for hand orthosis supported neuro-rehabilitation *J. Neurosci. Methods* **312** 1–11
- [21] Li S and Francisco G E 2015 New insights into the pathophysiology of post-stroke spasticity *Front. Hum. Neurosci.* **9** 192
- [22] Bhakta B B 2000 Management of spasticity in stroke *Br. Med. Bull.* **56** 476–85
- [23] Zhang X and Zhou P 2012 Sample entropy analysis of surface EMG for improved muscle activity onset detection against spurious background spikes *J. Electromyogr. Kinesiol.* **22** 901–7
- [24] Cai S, Li G, Su E, Wei X, Huang S, Ma K, Zheng H and Xie L 2020 Real-time detection of compensatory patterns in patients with stroke to reduce compensation during robotic rehabilitation therapy *IEEE J. Biomed. Health. Inf.* **24** 2630–8
- [25] Lalitharatne T D, Teramoto K, Hayashi Y and Kiguchi K 2013 Towards hybrid EEG-EMG-based control approaches to be used in bio-robotics applications: current status, challenges and future directions *Paladyn J. Behav. Robot.* **4** 147–54
- [26] Sarasola-Sanz A, Irastorza-Landa N, López-Larraz E, Bibián C, Helmhold F, Broetz D, Birbaumer N and Ramos-Murguialday A 2017 A hybrid brain-machine interface based on EEG and EMG activity for the motor rehabilitation of stroke patients *2017 Int. Conf. on Rehabilitation Robotics (ICORR)* (IEEE) pp 895–900
- [27] Williams E R, Soteropoulos D S and Baker S N 2009 Coherence between motor cortical activity and peripheral discontinuities during slow finger movements *J. Neurophysiol.* **102** 1296–309
- [28] Mima T, Toma K, Koshiy B and Hallett M 2001 Coherence between cortical and muscular activities after subcortical stroke *Stroke* **32** 2597–601
- [29] Guo Z, Qian Q, Wong K, Zhu H, Huang Y, Hu X and Zheng Y 2020 Altered corticomuscular coherence (CMCoh) pattern in the upper limb during finger movements after stroke *Front. Neurol.* **11** 410
- [30] Liu J, Sheng Y and Liu H 2019 Corticomuscular coherence and its applications: a review *Front. Hum. Neurosci.* **13** 100
- [31] Meng F, Tong K-Y, Chan S-T, Wong -W-W, Lui K-H, Tang K-W, Gao X and Gao S 2008 Cerebral plasticity after subcortical stroke as revealed by cortico-muscular coherence *IEEE Trans. Neural Syst. Rehabil. Eng.* **17** 234–43
- [32] Lattari E, Velasques B, Paes F, Cunha M, Budde H, Basile L, Cagy M, Piedade R, Machado S and Ribeiro P 2010

- Corticomuscular coherence behavior in fine motor control of force: a critical review *Rev. Neurol.* **51** 610–23
- [33] Wang Y, Xie P, Zhou S, Wang X and Yuan Y 2019 Low-intensity pulsed ultrasound modulates multi-frequency band phase synchronization between LFPs and EMG in mice *J. Neural Eng.* **16** 026036
- [34] Luft A R, Forrester L, Macko R F, McCombe-Waller S, Whitall J, Villagra F and Hanley D F 2005 Brain activation of lower extremity movement in chronically impaired stroke survivors *Neuroimage* **26** 184–94
- [35] Mima T, Steger J, Schulman A E, Gerloff C and Hallett M J C N 2000 Electroencephalographic measurement of motor cortex control of muscle activity in humans *Clin. Neurophysiol.* **111** 326–37
- [36] Kong K-H, Chua K S and Lee J 2011 Recovery of upper limb dexterity in patients more than 1 year after stroke: frequency, clinical correlates and predictors *NeuroRehabilitation* **28** 105–11
- [37] Folstein M F, Folstein S E and McHugh P R 1975 'Mini-mental state': a practical method for grading the cognitive state of patients for the clinician *J. Psychiatr. Res.* **12** 189–98
- [38] Fugl-Meyer A R, Jääskö L, Leyman I, Olsson S and Steglind S 1975 The post-stroke hemiplegic patient. 1. A method for evaluation of physical performance *Scand. J. Rehabil. Med.* **7** 13–31
- [39] Pandyan A D, Johnson G R, Price C I, Curless R H, Barnes M P and Rodgers H 1999 A review of the properties and limitations of the Ashworth and modified Ashworth Scales as measures of spasticity *Clin. Rehabil.* **13** 373–83
- [40] Hu X, Tong K, Tsang V S and Song R 2006 Joint-angle-dependent neuromuscular dysfunctions at the wrist in persons after stroke *Arch. Phys. Med. Rehabil.* **87** 671–9
- [41] Ye F, Yang B, Nam C, Xie Y, Chen F and Hu X 2021 A data-driven investigation on surface electromyography (sEMG) based clinical assessment in chronic stroke *Front. Neurobot.* **15** 94
- [42] Goodin P, Lamp G, Vidyasagar R, McArdle D, Seitz R J and Carey L M 2018 Altered functional connectivity differs in stroke survivors with impaired touch sensation following left and right hemisphere lesions *NeuroImage* **18** 342–55
- [43] Zhou S, Huang Y, Jiao J, Hu J, Hsing C, Lai Z, Yang Y and Hu X 2021 Impairments of cortico-cortical connectivity in fine tactile sensation after stroke *J. Neuroeng. Rehabil.* **18** 34
- [44] Yozbatiran N, Der-Yeghiaian L and Cramer S C 2008 A standardized approach to performing the action research arm test *Neurorehabil. Neural Repair* **22** 78–90
- [45] Divekar N V and John L R 2013 Neurophysiological, behavioural and perceptual differences between wrist flexion and extension related to sensorimotor monitoring as shown by corticomuscular coherence *Clin. Neurophysiol.* **124** 136–47
- [46] Bundy D T, Souders L, Baranyai K, Leonard L, Schalk G, Coker R, Moran D W, Huskey T and Leuthardt E C 2017 Contralateral brain-computer interface control of a powered exoskeleton for motor recovery in chronic stroke survivors *Stroke* **48** 1908–15
- [47] Pichiorri F et al 2015 Brain-computer interface boosts motor imagery practice during stroke recovery *Ann. Neurol.* **77** 851–65
- [48] Benzy V, Vinod A, Subasree R, Alladi S and Raghavendra K 2020 Motor imagery hand movement direction decoding using brain computer interface to aid stroke recovery and rehabilitation *IEEE Trans. Neural Syst. Rehabil. Eng.* **28** 3051–62
- [49] Qiuyang Q, Nam C, Guo Z, Huang Y, Hu X, Ng S C, Zheng Y and Poon W 2019 Distal versus proximal-an investigation on different supportive strategies by robots for upper limb rehabilitation after stroke: a randomized controlled trial *J. Neuroeng. Rehabil.* **16** 1–16
- [50] Marigold D S, Eng J J, Tokuno C D and Donnelly C A 2004 Contribution of muscle strength and integration of afferent input to postural instability in persons with stroke *Neurorehabil. Neural Repair* **18** 222–9
- [51] Boyaci A, Topuz O, Alkan H, Ozgen M, Sarsan A, Yildiz N and Ardic F 2013 Comparison of the effectiveness of active and passive neuromuscular electrical stimulation of hemiplegic upper extremities: a randomized, controlled trial *Int. J. Rehabil. Res.* **36** 315–22
- [52] Krebs H I, Volpe B T, Williams D, Celestino J, Charles S K, Lynch D and Hogan N 2007 Robot-aided neurorehabilitation: a robot for wrist rehabilitation *IEEE Trans. Neural Syst. Rehabil. Eng.* **15** 327–35
- [53] Yao J and Dewald J P A 2006 Cortico-muscular communication during the generation of static shoulder abduction torque in upper limb following stroke 2006 *Int. Conf. IEEE Engineering in Medicine and Biology Society* pp 181–4
- [54] Lai M-I, Pan L-L, Tsai M-W, Shih Y-F, Wei S-H and Chou L-W 2016 Investigating the effects of peripheral electrical stimulation on corticomuscular functional connectivity stroke survivors *Top Stroke Rehabil.* **23** 154–62
- [55] McPherson J G, Chen A, Ellis M D, Yao J, Heckman C and Dewald J P 2018 Progressive recruitment of contralateral cortico-reticulospinal pathways drives motor impairment post stroke *J. Physiol.* **596** 1211–25
- [56] Bao S-C, Wong W-W, Leung T W H and Tong K-Y 2018 Cortico-muscular coherence modulated by high-definition transcranial direct current stimulation in people with chronic stroke *IEEE Trans. Neural Syst. Rehabil. Eng.* **27** 304–13